Available online at www.sciencedirect.com
ScienceDirect
Polymer 47 (2006) 8350–8359
polymer
www.elsevier.com/locate/polymer

Miscibility with positive deviation in T_g–composition relationship in blends of poly(2-vinyl pyridine)-*block*-poly(ethylene oxide) and poly(*p*-vinyl phenol)

Li-Ting Lee [a], Eamor M. Woo [a,*], Sheng Shu Hou [a], Stephan Förster [b]

[a] *Department of Chemical Engineering, National Cheng Kung University, #1 University Road, Tainan 701-01, Taiwan*
[b] *Institute for Physical Chemistry, University of Hamburg, Grindelallee 117, 20146 Hamburg, Germany*

Received 8 June 2006; received in revised form 9 September 2006; accepted 7 October 2006
Available online 27 October 2006

Abstract

Phase behavior and miscibility with positive deviation from linear T_g–composition relationship in a copolymer/homopolymer blend system, poly(2-vinyl pyridine)-*block*-poly(ethylene oxide) (P2VP-*b*-PEO)/poly(*p*-vinyl phenol) (PVPh), were investigated by differential scanning calorimetry (DSC), Fourier-transform infrared spectroscopy (FT-IR) and solid-state ^{13}C nuclear magnetic resonance (^{13}C NMR), optical microscopy (OM), and scanning electron microscopy (SEM). Optical and electron microscopy results as well as NMR proton spin–lattice relaxation times in laboratory frame (T_1^H) all confirmed the miscibility as judged by the T_g criterion using DSC. In comparison to the literature result on a homopolymer/homopolymer blend of P2VP/PVPh, fitting with the Kwei equation on the T_g–composition relationship for the block-copolymer/homopolymer blend of P2VP-*b*-PEO/PVPh blend system yielded a smaller q value ($q = 120$) for P2VP-*b*-PEO/PVPh than that for P2VP/PVPh blend ($q = 160$). The FT-IR and ^{13}C NMR results revealed hydrogen-bonding interactions between the pendant pyridine group of P2VP-*b*-PEO and phenol unit in PVPh, which is responsible for the noted positive deviation of the T_g–composition relationship. Comparison of the shifts of hydroxyl IR absorbance band, reflecting the average strength of H-bonding, indicates a decreasing order of P2VP/PVPh > P2VP-*b*-PEO/PVPh > PEO/PVPh blends. The PEO block in the copolymer segment tends to defray the interaction strength in the P2VP-*b*-PEO/PVPh blends because of relative weaker interaction between PEO and PVPh than that between P2VP and PVPh pairs. A comparative ternary (P2VP/PEO)/PVPh blend was also studied as the controlling experiments for comparison to the P2VP-*b*-PEO/PVPh blend. The thermal behavior and interaction strength in (P2VP/PEO)/PVPh ternary blends are discussed with those in the P2VP-*b*-PEO/PVPh copolymer/homopolymer blend.

Keywords: Miscibility; P2VP-*b*-PEO block copolymer; Poly(*p*-vinyl phenol)

1. Introduction

Blends of polymers have attracted a lot of interests [1–12]. The main reason is that polymer blends provide convenience in custom-tailoring the physical or chemical properties by combining different polymeric materials for various end uses. Hydrogen bonding is one type of specific interaction in many miscible blends that comprise proton-donating and proton-accepting polymers [13]. Poly(*p*-vinyl phenol) (PVPh), which has a hydroxyl group at the pendant phenyl ring, is generally capable of interacting with proton-accepting functional groups in other polymers such as poly(trimethylene terephthalate) (PTT), poly(butylene adipate) (PBA) and poly(*N*,*N*-dimethyl acrylamide) (PDMA) [14–16]. Recent attentions are focused on the blends of PVPh with vinylpyridine-containing polymers, such as poly(2-vinyl pyridine)/PVPh (P2VP/PVPh) and poly(4-vinyl pyridine)/PVPh (P4VP/PVPh) blends. PVPh can form strong H-bonding interactions to both P2VP and P4VP. Furthermore, inter-polymer complexes may be produced by using methanol as the solvent for preparing the blends [17].

* Corresponding author. Tel.: +886 6 275 7575; fax: +886 6 234 4496.
E-mail address: emwoo@mail.ncku.edu.tw (E.M. Woo).

0032-3861/$ - see front matter © 2006 Elsevier Ltd. All rights reserved.
doi:10.1016/j.polymer.2006.10.005

In order to avoid formation of complexes between PVPh and P2VP or P4VP with aim to prepare normal physical blends, Goh et al. [18] and Wang et al. [19] modified the experimental procedure by using *N*,*N*-dimethylformamide (DMF) rather than methanol. DMF is a polar solvent that can simultaneously and evenly interact with PVPh and vinylpyridine-containing polymer. In addition, other blends have also been obtained in the literature by using pyridine as the solvent, which was based on the same principle in using DMF for preparing blends [17]. The T_g–composition relationship in PVPh/P2VP and PVPh/P4VP blends are interesting in that positive deviation of T_g–composition relationships have been observed in both systems, where strong H-bonding interactions are present between the constituent components in the blends [17–19].

Block copolymers have attracted attentions in the recent years because of their specific multi-phase morphology with interesting or useful self-assembly behavior. Förster and Bates [20,21] have been the first to demonstrate the phase diagrams for such block copolymers with experimental proofs. Amphiphilic block copolymers are those consisting of a block of hydrophobic polymer covalently linked to another block of hydrophilic polymer. The amphiphilic block copolymers exhibit characteristics similar to low-molecular-weight surfactants or lipids; and in aqueous solutions, they can possess capacity of self-assembly into various shapes such as micelle, vesicle, or lyotropic morphologies with potential applications in encapsulation or control release of substances [22]. Poly(2-vinyl pyridine)-*block*-poly(ethylene oxide) (P2VP-*b*-PEO) is an ''amphiphilic'' block copolymer, which has a water-insoluble P2VP block and water-soluble PEO block. Mayer and Förster have demonstrated a vesicle-like morphology in P2VP-*b*-PEO block copolymers and their permeability properties by using PFG-NMR [23]. In this study, P2VP-*b*-PEO was used as a model copolymer for blending with PVPh in aims to understand effects of such amphiphilic block segments on interactions, miscibility, and morphology. Various techniques of characterization were performed to reveal the thermal behavior, specific interactions, and miscibility in the blends of the amphiphilic block copolymer of P2VP-*b*-PEO/PVPh with hydroxyl-containing PVPh. PVPh is known to interact with both P2VP and PEO segments, but interactions may differ with these two blocks. Comparisons were also made between the P2VP-*b*-PEO copolymer/PVPh blend with P2VP/PVPh blend that has been reported in the literature [18]. Relevant analyses were performed in attempts to understand the influence of PEO block on the thermal, phase morphology, and specific interactions.

2. Experimental part

2.1. Materials and preparation

Poly(*p*-vinyl phenol) (PVPh with $M_w = 22{,}000\ g\ mol^{-1}$) was supplied from Polysciences Inc. (USA). Block copolymer, poly(2-vinyl pyridine)-*block*-poly(ethylene oxide) (P2VP-*b*-PEO), was synthesized by sequential living anionic polymerization of 2-vinylpyridine and ethylene oxide initiated by diphenylmethyl-potassium in THF as described earlier [24]. The block copolymer was characterized by GPC, NMR and MALDI-TOF-MAS and has degrees of polymerization of N(P2VP) = 55 and N(PEO) = 38 with polydispersity of $M_w/M_n = 1.08$. PVPh is an amorphous polymer with $M_w = 22{,}000\ g\ mol^{-1}$, which was obtained from Polysciences, Inc. (USA). A solution-blending procedure was adopted for sample preparation. Polymers in *N*,*N*-dimethylformamide (DMF) solutions containing 4 wt% polymer species of different P2VP-*b*-PEO to PVPh ratios were prepared and then cast onto either glass or aluminum substrates at 50 °C for 48 h. Afterwards, the as-cast films were moved to a vacuum oven with temperature control at 120 °C for 4 days in order to remove residual solvent before measurements. In order to compare with the block-copolymer blends, the homopolymer ternary blend of (P2VP/PEO)/PVPh was also investigated. The P2VP ($M_w = 5300\ g\ mol^{-1}$) and PEO ($M_w = 1500\ g\ mol^{-1}$) with lower molecular weights used were obtained from Aldrich Inc. The molecular weights of P2VP and PEO were selected to approach the blocking molecular weights of the P2VP and PEO blocks in the P2VP-*b*-PEO block copolymer in this study. The weight ratio of P2VP/PEO in the ternary blends was fixed at 77/22, which is nearly the weight ratio of P2VP block to PEO block in the P2VP-*b*-PEO block copolymer. The preparation method for homopolymer (P2VP/PEO)/PVPh ternary blends was similar with that for the copolymer P2VP-*b*-PEO/PVPh blends. For direct comparison, the ratio of P2VP/PEO in the ternary homopolymer blends was fixed at 77/22, which is same as the weight ratio of these two segments in the P2VP-*b*-PEO copolymer.

2.2. Differential scanning calorimetry

The glass transition temperatures of blends were characterized with a differential scanning calorimeter (Perkin–Elmer DSC-7) equipped with an intracooler. All T_g measurements were made at a scan rate of 20 °C/min within the range of −70 to 200 °C, and the T_g values were taken as the onset of the transition (i.e. the change of the specific heat) in the DSC thermograms. After the thermal scan experiments, obtained T_g values were also plotted against the blends' compositions for investigating the T_g–composition relationships of the blends.

2.3. Infrared spectroscopy

Fourier-transform infrared spectroscopy (FT-IR, Nicolet Magna-560) was used for exploring the interactions in the blends. Spectra were obtained at 4 cm^{-1} resolution at the average of 64 scans in the standard wavenumber range of 400–4000 cm^{-1}. All FT-IR samples were cast as thin films of proper thickness directly on KBr pellets kept at 50 °C. Note that measurements were carried out at room temperature and all film samples for IR were experimentally acceptable to obey the Beer–Lambert law for qualification analysis.

2.4. Optical and scanning electron microscopies

An optical microscope (Nikon Optiphot-2, POL) was used for observing the morphology in the blends. Before the examinations with the optical microscope (OM), as-cast blends were spread as thin films on glass slides and dried properly in a temperature-controlled oven. Blend samples were also examined using a scanning electron microscope (SEM, model: JEOL JXA840) for greater magnification on phase domains. Blend samples of two different thickness scales were prepared. Thick samples for SEM were prepared by melting in the DSC cells, which were removed from the aluminum cell after thermal treatments and were fractured across the thickness. Blend samples of thin films were obtained by solvent-casting (and evaporation) directly onto DSC aluminum pan or lid, which served as a conductive substrate for electron flow.

2.5. Solid-state NMR measurements

All NMR experiments were performed on a Bruker AVANCE-400 spectrometer at resonance frequencies of 100.62 MHz for ^{13}C and 400.13 MHz for ^{1}H, using a double-resonance magic-angle spinning (MAS) probe with 7 mm o.d. rotors. The ^{13}C NMR chemical shifts were externally referenced to tetramethylsilane (TMS). For the CP/MAS (cross-polarization from ^{1}H to ^{13}C) experiments, CP contact time was 1 ms and the recycle delay was 4 s. The spinning speed was 6.2 kHz in order to separate the obscuring spinning side bands from the resonance peaks of aromatic carbons. The T_1^H relaxation times were measured by the ^{1}H inversion-recovery experiment (180°-pulse-τ_{recov}-90°-pulse), with ^{13}C detection using the CP pulse sequence.

3. Results and discussion

3.1. Miscibility with T_g–composition relationship in P2VP-b-PEO/PVPh blends

DSC experiments performed for investigating the miscibility of P2VP-*b*-PEO/PVPh blends clearly revealed only a single and composition-dependent T_g for all 10 blend compositions, and all T_g transitions were reasonably sharp and not broadened. All traces show a reasonable sharp T_g transition dependent on composition; however, the graph for blend DSC traces are not shown for brevity. The neat P2VP-*b*-PEO copolymer also exhibits a single T_g, owing to small segment lengths with good intra-molecular mixing between the P2VP and PEO blocks in P2VP-*b*-PEO molecules. For comparison, in a concurrent study [25], miscibility was proven to exist between two homopolymers of P2VP and PEO of molecular weights equivalent to those in the copolymer segments. In addition, with increasing PVPh content in the blends (from top to bottom in the figure), the single T_g for each blend increases steadily with the composition. By the conventional T_g criterion, the DSC results clearly demonstrate that the blends with different compositions investigated here are all miscible, with an intimately mixing state among three polymeric segments of P2VP, PEO and PVPh in the blends.

The T_g's values of P2VP-*b*-PEO/PVPh blends are also re-plotted again with respect to the PVPh composition. Fig. 1 reveals the T_g–composition relationship for the P2VP-*b*-PEO/PVPh blends. Additionally, the data of P2VP/PVPh blends from the literature [18] are also attached in the same figure for comparison. It is clear that positive deviation from the linearity rule is apparent in the T_g–composition curves for the P2VP-*b*-PEO/PVPh blend as well as P2VP/PVPh blend system. The main factor for such positive deviation for the P2VP-*b*-PEO/PVPh blends is usually attributed to strong H-bonding interactions between P2VP and PVPh. Further evidence and discussions for the H-bonding in the P2VP-*b*-PEO/PVPh blends will be made in later sections of IR and ^{13}C NMR spectroscopy characterizations. The T_g–composition relationship can well be described by the Kwei equation [26,27] as Eq. (1), which is widely used for characterizing T_g's behavior in polymer blends with specific interactions. The Kwei equation is shown as follows:

$$T_g = \frac{W_1 T_{g1} + kW_2 T_{g2}}{W_1 + kW_2} + qW_1W_2 \quad (1)$$

where W_1 and W_2 are weight fractions of the components in the blends, T_{g1} and T_{g2} represent the corresponding glass transition temperatures, and k and q are fitting parameters. Note that the first term on the right-hand side of Eq. (1) is the widely used Gordon–Taylor equation, which can be derived formally by using the additive rule of the entropy or the volume of the mixtures. Besides, the second quadratic term qW_1W_2 is proportional to the strength of hydrogen bonding or specific interaction in the blends. The fitting led to a result of $k = 1$ and $q = 120$, as estimated by the Kwei equation, for the P2VP-*b*-PEO/PVPh blends. In the figure, relationship is

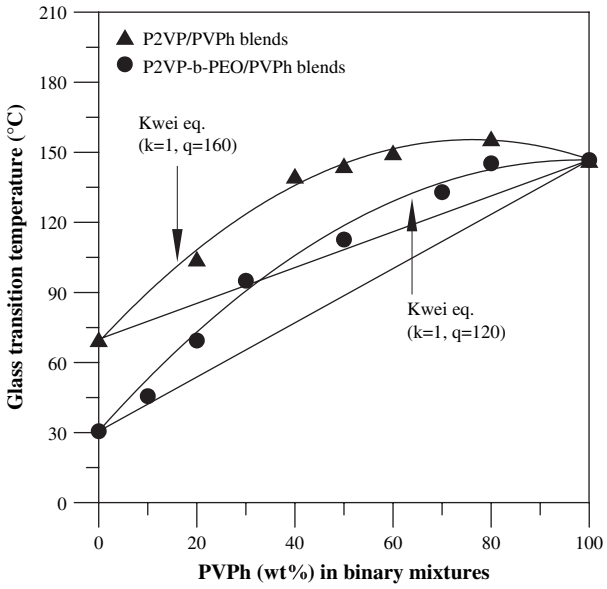

Fig. 1. T_g–composition relationship for the P2VP-*b*-PEO/PVPh and P2VP/PVPh blends and fitting with the Kwei equation.

shown for comparison, where calculation was based on $k = 1$ and $q = 160$ with the T_g data for the P2VP/PVPh system taken from the literature [18]. Less positive deviation is seen in the P2VP-*b*-PEO/PVPh blends, in comparison to the similarly positive deviation for the P2VP/PVPh blend system [18], which reflects that interactions are stronger in the latter blend system (i.e., P2VP/PVPh blend). The PEO block in the copolymer plays a role to reduce the interaction strength, which is apparent from the smaller q value ($q = 120$) for the P2VP-*b*-PEO/PVPh blend than that ($q = 160$) for the P2VP/PVPh blend. In addition, the T_g–composition relationship for the PEO/PVPh binary blends does not exhibit a positive deviation from linearity as do the P2VP-*b*-PEO/PVPh and P2VP/PVPh blend systems because of the relative weaker interactions between PEO and PVPh. A typical negative deviation from linearity for the T_g–composition relationship of PEO/PVPh has been addressed by Pedrosa et al. [28].

3.2. Spectroscopy characterization on interactions in blends

As discussed earlier on the thermal analysis result, there should be specific interactions leading to the noted positive deviation from linear T_g–composition relationship for the P2VP-*b*-PEO/PVPh blend. Additionally, FT-IR and ^{13}C NMR spectroscopy techniques were performed on the blends. FT-IR characterization was intended to explore the interactions in the P2VP-*b*-PEO/PVPh blends for qualitative and quantitative aspects. Fig. 2 demonstrates the IR absorption spectra for wavenumber regions of (A) 975–1030 cm^{-1} and (B) 3000–3700 cm^{-1} with different compositions in the P2VP-*b*-PEO/PVPh blends. In accordance with the literature studies [18,29], some characteristic modes of the pyridine ring are sensitive to the specific interactions, for example, 625, 993, 1050, and 1590 cm^{-1} bands.

However, owing to inevitable complication of overlapping by the PVPh absorption bands, only the band at 993 cm^{-1} can be used to identify the existence of interactions involving the pyridine groups. Fig. 2 illustrates IR spectra in two regions of (A) 975–1030 cm^{-1} and (B) hydroxyl-stretching band at 3000–3700 cm^{-1}, for different compositions of the P2VP-*b*-PEO/PVPh blends. Fig. 2(A) shows three IR bands at 993, 1005 and 1014 cm^{-1} with reasonable resolution. The 993 and 1014 cm^{-1} bands can be attributed to the aryl CH bending of P2VP pyridine group and PVPh phenol group, respectively [30]. The absorption at 1005 cm^{-1} is resulted from contribution of the strong hydrogen bonding between pyridine ring of P2VP and phenol group of PVPh, which has been earlier demonstrated in a homopolymer blend of P2VP/PVPh [18], where the 1005 cm^{-1} band has been suggested to imply H-bonding influence on coupled-CH bending between the pyridine ring and phenol group. In other words, the H-bonding

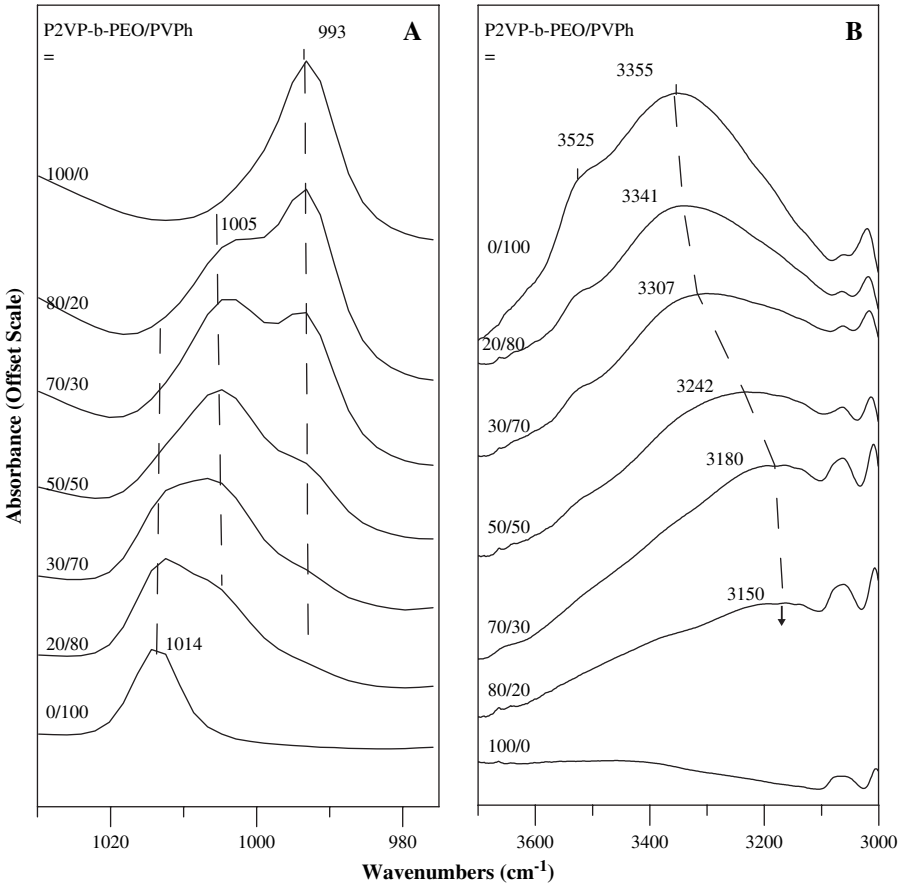

Fig. 2. IR absorption spectra for wavenumber regions of (A) 975–1030 cm^{-1} and (B) 3000–3700 cm^{-1} with different compositions in P2VP-*b*-PEO/PVPh blends.

interactions occur between the pendant pyridine group of P2VP-*b*-PEO and phenol group of PVPh, and the interactions play an important role in the noted positive deviation from linear T_g–composition relationship for the P2VP-*b*-PEO/PVPh blend. By comparison, Fig. 2(B) depicts the hydroxyl-stretching band at 3000–3700 cm^{-1} of the PVPh component in the P2VP-*b*-PEO/PVPh blend. Two distinct IR absorbance bands in the hydroxyl-stretching region are seen. A broad band at 3355 cm^{-1} can be attributed to the hydrogen-bonded hydroxyl group (self-association), and a relatively narrow band at 3525 cm^{-1} is assigned to the free (non-associated) hydroxyl groups [13]. Upon mixing with P2VP-*b*-PEO, the intensity of the free hydroxyl group band decreases and the hydrogen-bonded hydroxyl group band of PVPh shifts to a lower wavenumber (from 3355 to 3150 cm^{-1}). The spectral results in both wavenumber regions suggest that strong hydrogen-bonding interactions between the P2VP pyridine group and the PVPh phenol group leading to positive deviation from linear T_g–composition relationship in the P2VP-*b*-PEO/PVPh blend.

However, influence of PEO block on the strength of H-bonding interactions in the P2VP-*b*-PEO/PVPh blend can be observed by further analyzing the hydroxyl-stretching band. Coleman et al. [31] have employed a term of frequency difference ($\Delta\nu$) between the free hydroxyl group and those of the hydrogen-bonded hydroxyl groups as a measure of the average strength of H-bonding interactions in the blends. This method was also used and their procedures followed for estimating the H-bonding strength of the P2VP-*b*-PEO/PVPh blends. Table 1 summarizes the $\Delta\nu$ values for P2VP-*b*-PEO/PVPh blends and the other two H-bonded systems, i.e., P2VP/PVPh [18] and PEO/PVPh [31] blends. By analyzing the results, two findings may be apparent. First, the $\Delta\nu$ value of the P2VP-*b*-PEO/PVPh blend is intermediate between those for the P2VP/PVPh and PEO/PVPh blends. This fact reflects that both P2VP and PEO blocks of the P2VP-*b*-PEO copolymer interact with PVPh, but probably with unequal strengths. Secondly, the average strengths of H-bonding interactions are in a decreasing order of P2VP/PVPh ($\Delta\nu = 390\ cm^{-1}$) > P2VP-*b*-PEO/PVPh ($\Delta\nu = 365\ cm^{-1}$) > PEO/PVPh ($\Delta\nu = 325\ cm^{-1}$). This is consistent with the DSC result, which similarly suggests that the interactions in the P2VP-*b*-PEO/PVPh blend are weaker than those in the P2VP/PVPh blend. The PEO block reduces the H-bonding strength in the P2VP-*b*-PEO/PVPh blend because of the relative weaker H-bonding with PVPh in comparison to that between P2VP and PVPh.

To further confirm the interaction nature between P2VP-*b*-PEO and PVPh, one-dimensional (1D) solid-state ^{13}C NMR experiments were performed. Fig. 3 shows the ^{13}C CP-MAS spectra of neat PVPh, P2VP-*b*-PEO/PVPh (50/50) blend, and P2VP-*b*-PEO. Assignment of resonance peaks to various different carbons in the polymer is indicated in the figure, and the star symbols denote spinning side bands due to MAS. By comparing the ^{13}C spectrum of the blend with those of PVPh and P2VP-*b*-PEO, it can be seen that the carbons of phenol and pyridine rings have different chemical shift values from those of the pure constituent polymers (Table 2). The chemical shift of the aromatic ring carbons is very sensitive to its chemical environment induced by the circulation of the π electrons in the ring; therefore, variations of the resonance structure of an aromatic ring will lead to changes in the chemical shifts of ring carbons. Table 2 shows that the peaks of the carbon at 2 (C_i) and 6 (C_j) positions move upfield for the blend. This is because that the nitrogen of pyridine group forms a hydrogen bond with the proton of phenol group, through which it creates a partial positive charge on the nitrogen. This kind of interaction withdraws electron density from the ring and thus results in an upfield shift of the resonance peaks of the carbons bonded to the nitrogen. However, the peak of the carbon at 5-position (C_k), in *meta*-position to nitrogen, shifts downfield by 4.9 ppm. This is probably due to that the resonance structure has been altered by the strong hydrogen-bonding interaction and the intimate contact between the pyridine and phenol rings, and therefore it induces changes in the chemical environment of the carbon. The 1D CP-MAS NMR experiments confirm that the interaction in the P2VP-*b*-PEO/PVPh blend occur mainly between the pendant ring of P2VP-*b*-PEO and PVPh. The changes in chemical shifts of the ring carbons in P2VP block and PVPh are also in agreement with the results obtained from the FT-IR study, in which the absorption bands at 993 cm^{-1} (P2VP) and 1014 cm^{-1} (PVPh) resulted from ring stretching vibrations are perturbed by the hydrogen-bonding interaction and shift to 1005 cm^{-1}.

The segmental scale of blend miscibility could also be examined with techniques of dynamic relaxation experiments through ^{13}C NMR CP-MAS. By determining the proton relaxation time values for the neat component polymers, it may be possible to estimate an upper limit to the scale of heterogeneity in the blend. If the scale of the phase separation in the blend is sufficiently small to permit rapid diffusion of proton spin energy, a single-component relation process is observed. The measurement T_1^H provides information about the domains smaller than 100 nm. In the T_1^H experiments, the inversion-recovery method was used. The intensities of various carbon resonances of neat P2VP-*b*-PEO, PVPh and P2VP-*b*-PEO/PVPh blends were measured as a function of delay time, where various delay times were introduced between the $\pi/2$ and π pulses. According to the method used, the magnetization of resonances that relax at a single exponential function should obey the following equation:

$$M(\tau) = M_0\left[1 - 2\exp\left(-\tau/T_1^H\right)\right] \quad (2)$$

where τ is the delay time used in the experiment and $M(\tau)$ is the corresponding resonance intensity; M_0 is the intensity of

Table 1
Wavenumber shift ($\Delta\nu$) of OH stretching region in three blends comprising PVPh

Blends	$\Delta\nu$ (cm^{-1})
P2VP/PVPh	390[a]
P2VP-*b*-PEO/PVPh	365
PEO/PVPh	325[b]

[a] Ref. [18].
[b] Ref. [31].

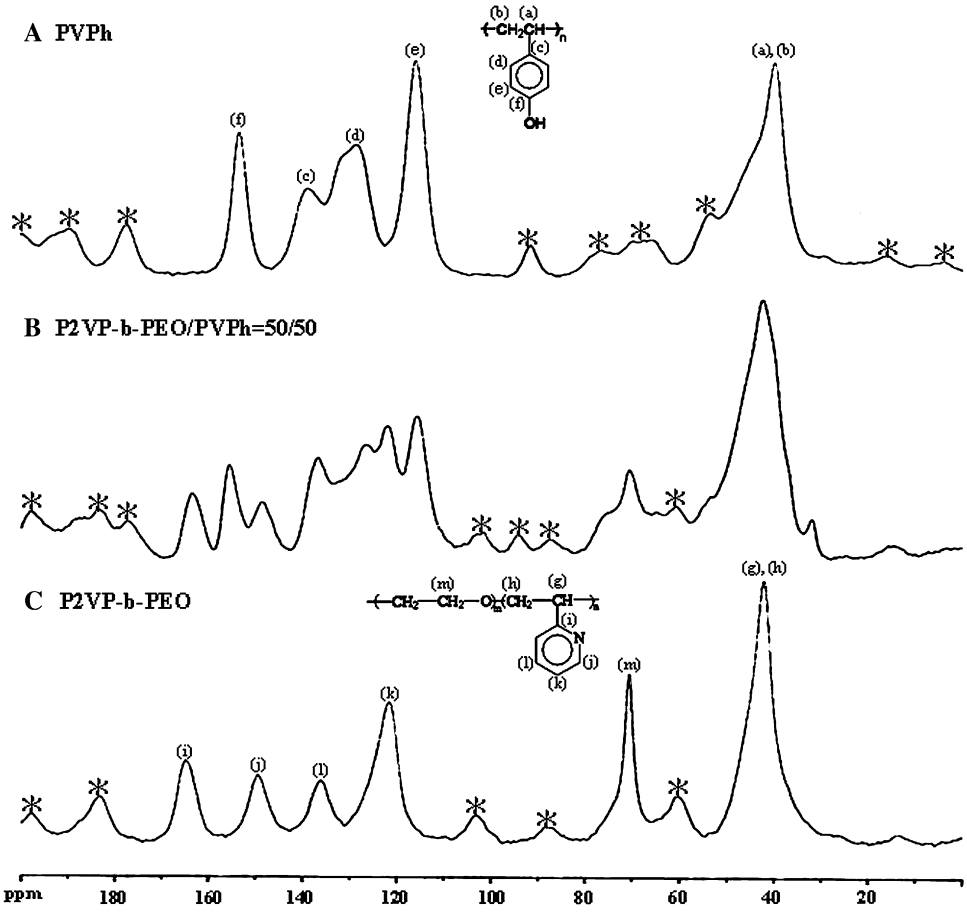

Fig. 3. ^{13}C CP-MAS NMR spectra of P2VP-*b*-PEO/PVPh blends of (A) PVPh, (B) P2VP-*b*-PEO/PVPh = 50/50, and (C) P2VP-*b*-PEO at room temperature and at a spinning speed of 6.2 kHz; peak assignment as indicated in figure.

the resonance at $\tau \geq 5T_1^H$. Taking the natural logarithm of both sides of Eq. (2), the following relationship can thus be obtained:

$$\ln\left[\frac{M_0 - M(\tau)}{2M_0}\right] = \frac{-\tau}{T_1^H} \tag{3}$$

From this equation, the left-hand term $\ln[M_0 - M(\tau)/2M_0]$ was plotted versus delay time τ to yield values of T_1^H.

Table 2
Difference in ^{13}C chemical shifts for the pure PVPh, P2VP-*b*-PEO and P2VP-*b*-PEO/PVPh blend

Carbons	PVPh (ppm)	P2VP-*b*-PEO (ppm)	P2VP-*b*-PEO/PVPh = 50/50 (ppm)	Δ, ppm[a]
C_f	153.2	–	155.3	−2.1
C_c	138.6	–	136.4	+2.2
C_d	128.3	–	126.5	+1.8
C_e	115.7	–	116.6	−0.9
C_i	–	164.7	163.4	+1.3
C_j	–	149.4	148.5	+0.9
C_k	–	121.6	126.5	−4.9

[a] The sign indicates an upfield shift (+) and an downfield shift (−) for the carbons in the blend, as compared to the pure constitute polymers.

As depicted in Fig. 4, all the ^{13}C resonance intensities of neat P2VP-*b*-PEO, PVPh, and their blends show a single exponential decay. Additionally, the logarithmic plots of ^{13}C resonance intensity $M(\tau)$ versus delay time τ for the selected carbon of neat P2VP-*b*-PEO, neat PVPh, and their 50/50 blend all show a linear relationship.

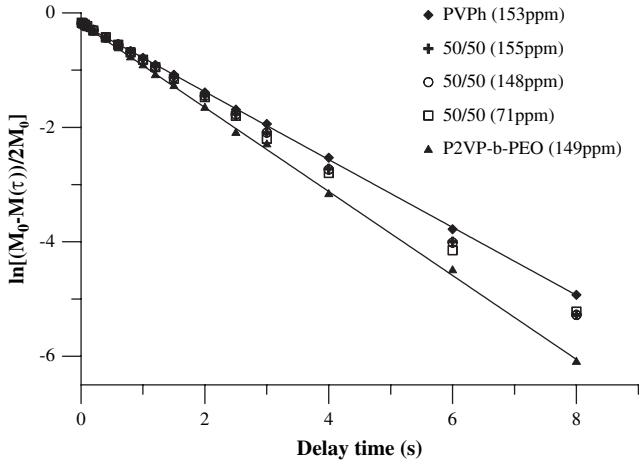

Fig. 4. Logarithmic plot of ^{13}C NMR resonance intensities as a function of delay time for PVPh, P2VP-*b*-PEO, and the 50/50 blend at room temperature. The slope yields the proton spin–lattice relaxation time in the laboratory frame T_1^H.

Table 3
T_1^H values of P2VP-*b*-PEO/PVPh at room temperature

P2VP-*b*-PEO/PVPh blends (wt%)	PVPh T_1^H (s)		P2VP T_1^H (s)		PEO T_1^H (s)
	153 ppm	115 ppm	149 ppm	121 ppm	70 ppm
0/100	1.69	1.65	–	–	–
50/50	1.57	1.56	1.57	1.54	1.53
100/0	–	–	1.26	1.28	1.23

The T_1^H values obtained from Eq. (3) for the neat P2VP-*b*-PEO, PVPh, and their blends are summarized in Table 3. These values were measured at 149, 121 and 70 ppm for P2VP-*b*-PEO, or at 153 and 115 ppm for PVPh. Single-component-dependent T_1^H was obtained for all specimens here. An examination of the experimental T_1^H data shows that the various carbon signals for both neat polymers exhibit nearly the same T_1^H values. Although there is no major difference between the T_1^H values of P2VP-*b*-PEO and PVPh, it is apparent that the relaxation processes for the blends are intermediate in their values when compared to those for the neat components. The fact of a single T_1^H indicates that the spin diffusion process is sufficiently fast to equilibrate the relaxation times for all protons among the chemically different constituents, and the studied blends are completely homogeneous on the time scale of T_1^H.

In addition, a useful approximate estimation of the upper limit to the domain size can be made with the following equation [32,33]:

$$\langle L\rangle \cong \left(6DT_i^H\right)^{1/2} \tag{4}$$

where $\langle L\rangle$ is the average diffusive path length for the effective spin diffusion, D is the spin diffusion coefficient. Typically, D is about 0.8 $nm^2\,ms^{-1}$ in a rigid proton system [32] and this value is also used in the calculation of this study. By using Eq. (4) with the T_1^H value of the 50/50 blend listed in Table 3, it becomes apparent that the P2VP-*b*-PEO/PVPh blends are intimately mixed on the upper limit of $\langle L\rangle \sim 87$ nm. Since the single-T_g criterion from DSC measurement usually demonstrates a miscible scale of 10–30 nm for the blends, the present NMR results show that the domain size is smaller than 87 nm and the results also support the miscibility as proven by the single-T_g criterion.

3.3. Morphological evidences of miscibility in P2VP-b-PEO/PVPh blends

Blend morphology was characterized. Cast thin-film blend samples, as well as fractured surface of bulk blend samples, were examined using OM and SEM for different levels of magnification. Fig. 5 shows the OM and SEM morphologies for cast thin-film blend samples: (A) P2VP-*b*-PEO/PVPh = 70/30 and (B) P2VP-*b*-PEO/PVPh = 30/70. All specimens were first observed by using OM at 800×. The OM graphs in Fig. 6 (top two graphs) are clear with no domains,

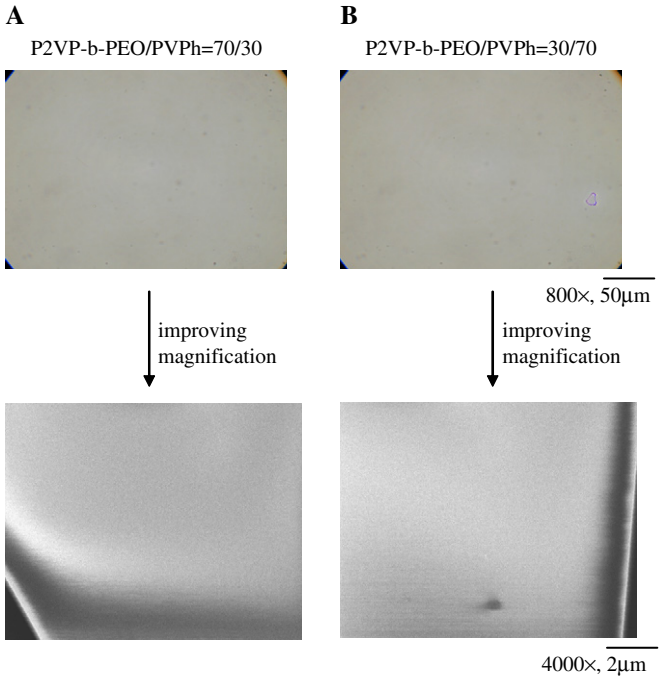

Fig. 5. OM and SEM morphologies for thin-film samples of (A) P2VP-*b*-PEO/PVPh = 70/30 and (B) P2VP-*b*-PEO/PVPh = 30/70 specimens.

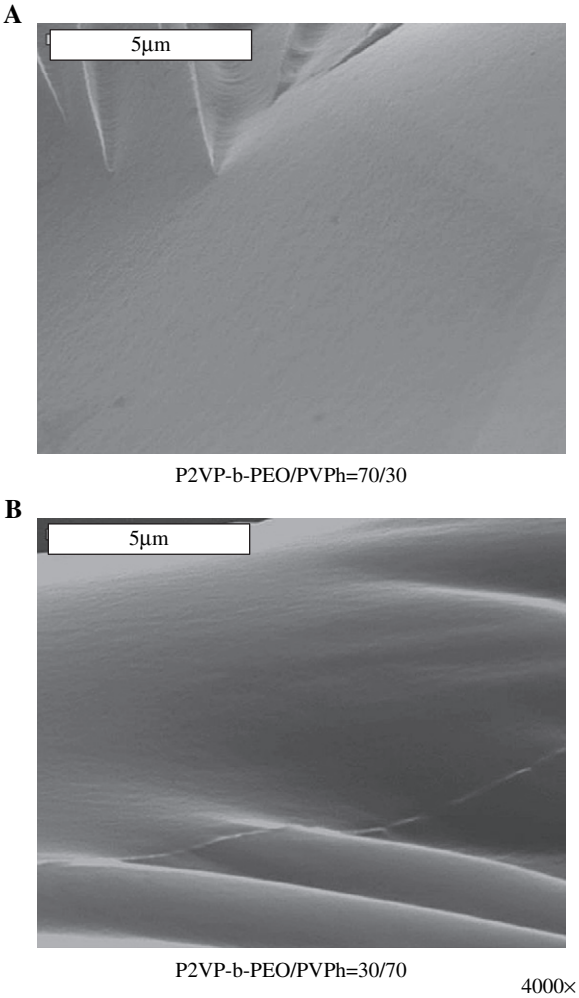

Fig. 6. SEM images of fractured surface in bulk-state samples of (A) P2VP-*b*-PEO/PVPh = 70/30 and (B) P2VP-*b*-PEO/PVPh = 30/70 specimens.

proving homogeneity for the P2VP-*b*-PEO/PVPh blends at the OM resolution. Similar homogeneous morphology at greater magnification (4000×) by SEM (bottom two graphs) for the blend surfaces also supports the conclusion of absence of any discernible phase domains in the blend systems.

In addition to the thin-film surface morphology, SEM characterization on the fractured surfaces of the bulk samples of the P2VP-*b*-PEO/PVPh blends was comparatively performed. Fig. 6 displays the images of fractured surface in bulk-like samples of (A) P2VP-*b*-PEO/PVPh = 70/30 and (B) P2VP-*b*-PEO/PVPh = 30/70 specimens. Domains of any phase heterogeneity are either absent or unable to be detected on the P2VP-*b*-PEO/PVPh blends. The fractured surfaces of P2VP-*b*-PEO/PVPh blends display lack of any phase-separation domains, which is similar to morphology homogeneity for the thin-film blend samples. Both OM and SEM morphology results justify and agree with the DSC result of miscibility in these blends.

To summarize the evidence by DSC, IR, ^{13}C NMR, OM and SEM characterizations, effects of the PEO segment on the intermolecular interactions can be better visualized by a schematic drawing. Fig. 7 shows a schematic for the chain-segment interactions leading to positive deviation from a linear T_g–composition relationship for the miscibility in the P2VP-*b*-PEO/PVPh blends. Three types of chain-segment interactions likely exist. Type (I) demonstrates P2VP segmental units strongly H-bonded with the PVPh phenol group. Type (II) illustrates inter- or intra-molecular mixing/entanglement between the P2VP and PEO segments. In addition, Type (III) depicts the PEO component that exerts relatively weaker H-bonding strength with the PVPh phenol group. Type (I) may be the major factor in leading to positive deviation from linear T_g–composition relationship in the P2VP-*b*-PEO/PVPh blend. By comparison, as shown in Type (III), the relatively weaker H-bonding between PEO and PVPh is responsible for the slightly lower average interaction strength in the P2VP-*b*-PEO/PVPh blend.

3.4. (P2VP/PEO)/PVPh ternary blends

PVPh is miscible with P2VP or PEO homopolymers [18,28] and its miscibility with a block copolymer, P2VP-*b*-PEO, is also proven in this study. Thus, ternary miscibility in P2VP/PEO/PVPh blends might be worth probing. The T_g criterion was used to characterize the miscibility in the ternary (P2VP/PEO)/PVPh blends. It has to emphasize that the weight ratio of P2VP/PEO in the ternary blends was at 77/22, which is also the weight ratio of P2VP block to PEO block in the P2VP-*b*-PEO block copolymer. DSC experiments performed for studying the miscibility of P2VP-*b*-PEO/PVPh blends revealed only a single and composition-dependent T_g for all compositions investigated here. This result provides evidence for proving miscibility in the (P2VP/PEO)/PVPh ternary blends. All traces show a sharp T_g transition dependent on composition; however, the graph for blend DSC traces are not shown for brevity. The T_g–composition relationship for the blends is presented in Fig. 8. For reference, the inset diagram in the figure shows the respective DSC traces of blends, from which single and composition-dependent T_g for the blends of all composition is apparent. The relationship as plotted shows a positive deviation from linearity for the (P2VP/PEO)/PVPh

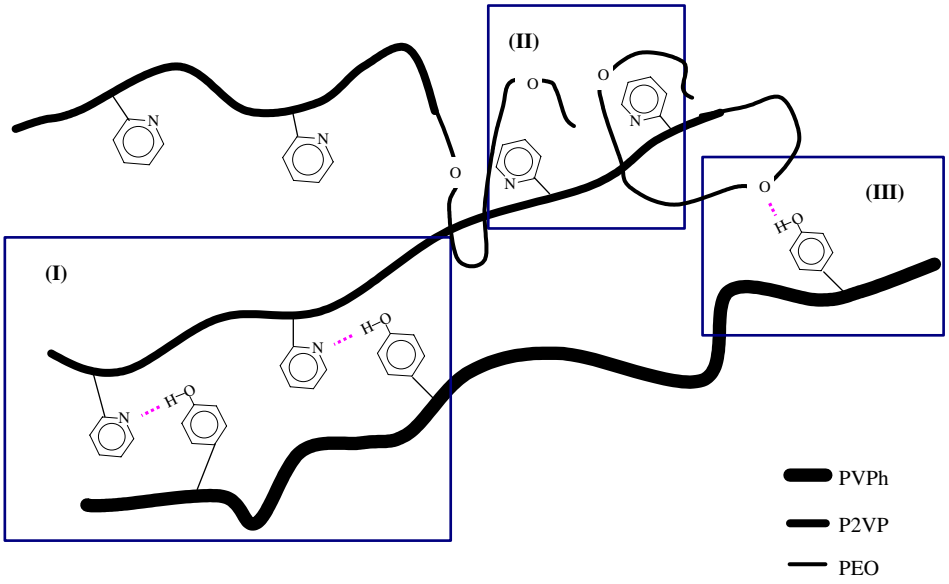

(I) H-bonding between P2VP and PVPh segments

(II) Inter- or intra-molecular mixing/entanglements between P2VP and PEO segments

(III) H-bonding between PEO and PVPh segments

Fig. 7. Illustration of relationships among P2VP, PEO and PVPh segments in P2VP-*b*-PEO/PVPh blends.

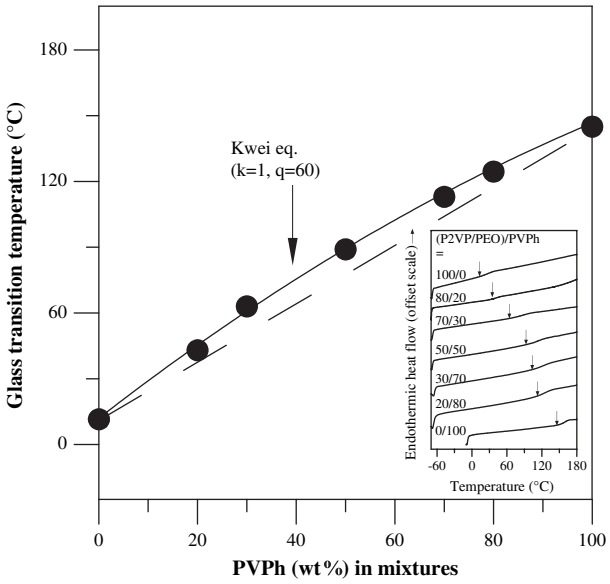

Fig. 8. T_g–composition relationship for (P2VP/PEO)/PVPh blends and fitting with the Kwei T_g model. Inset: DSC traces of blends.

blend, which is also seen in the P2VP-*b*-PEO/PVPh blends. The T_g data of the blends were also fitted by the Kwei equation, leading to $k = 1$ and $q = 60$, for the ternary (P2VP/PEO)/PVPh blends. Such positive deviation, though with a smaller q for the ternary (P2VP/PEO)/PVPh blends, again is usually attributed to H-bonding interactions between P2VP and PVPh.

3.5. IR characterization on (P2VP/PEO)/PVPh ternary blends

As demonstrated earlier on the thermal analysis investigation, there should be specific interactions leading to the positive deviation from linear T_g–composition relationship for the (P2VP/PEO)/PVPh blend. Further evidence for the H-bonding in the (P2VP/PEO)/PVPh blends was sorted by using IR spectroscopy. Fig. 9 shows IR absorption spectra for different wavenumber regions of (A) 970–1030 cm^{-1}, and (B) 3000–3800 cm^{-1} with different weight ratios in the (P2VP/PEO)/PVPh blends. Fig. 9(A) demonstrates three bands at 992, 1005 and 1014 cm^{-1} with reasonable resolution. The 992 and 1014 cm^{-1} bands are resulted from the aryl CH bending of P2VP pyridine group and PVPh phenol group, respectively. The absorption at 1005 cm^{-1} is considered as contribution of coupled-CH vibration owing to hydrogen bonding between pyridine ring of P2VP and phenol group of PVPh. By comparison, Fig. 9(B) reveals the hydroxyl-stretching band at 3000–3700 cm^{-1} of the PVPh component in the (P2VP/PEO)/PVPh blend. Upon mixing with (P2VP/PEO), the intensity of the free hydroxyl group band decreases and the hydrogen-bonded hydroxyl group band of PVPh shifts to a lower

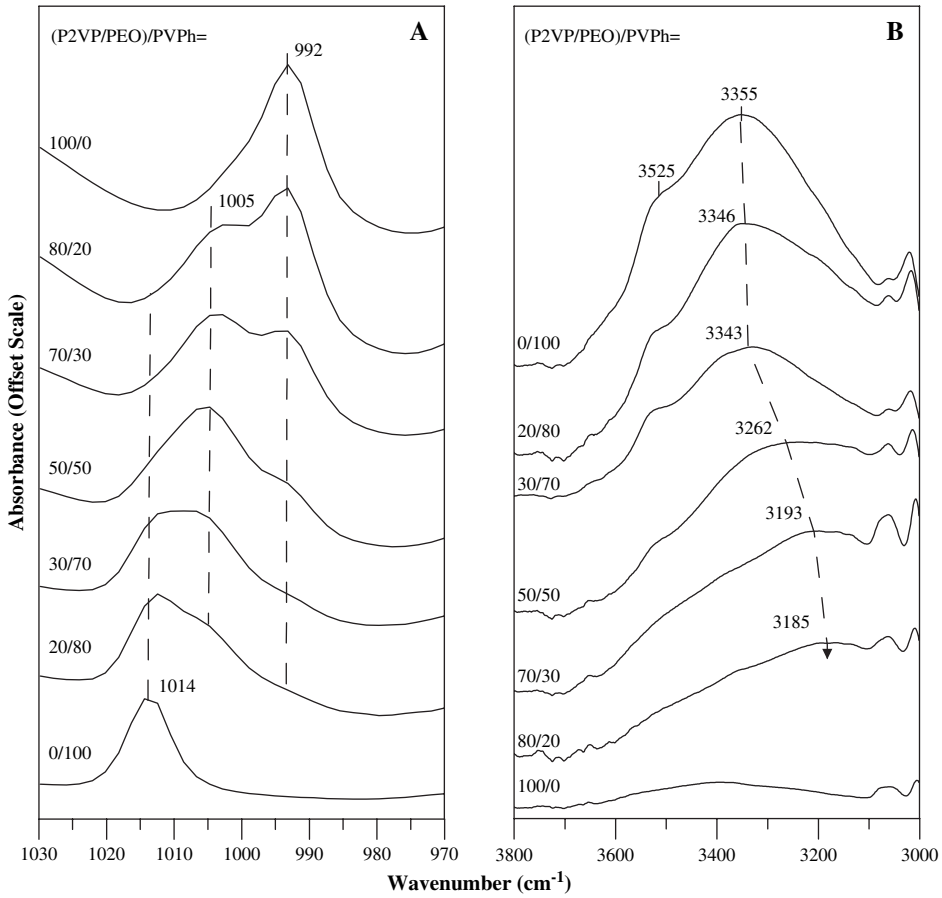

Fig. 9. IR absorption spectra for wavenumber regions: (A) 970–1030 cm^{-1} and (B) 3000–3700 cm^{-1} for the (P2VP/PEO)/PVPh blends of different weight ratios.

wavenumber (from 3355 to 3185 cm^{-1}), indicating the H-bonding interactions in the blends. All spectral features for (P2VP/PEO)/PVPh are similar with those for P2VP-*b*-PEO/PVPh blends. The spectral results suggest that specific hydrogen-bonding interactions are apparent in the ternary (P2VP/PEO)/PVPh blends, leading to positive deviation from linearity in the T_g–composition relationship.

4. Conclusions

Blends of a P2VP-*b*-PEO copolymer with PVPh homopolymer were proven to be miscible with specific interactions between the homopolymer and copolymer segments, leading to positive deviation from linear T_g–composition relationship. The Kwei equation reasonably describes the T_g–composition relationship for P2VP-*b*-PEO/PVPh blends with $q = 120$, which is smaller than that ($q = 160$) for the P2VP/PVPh blends. In general, the average specific interactions in the P2VP-*b*-PEO/PVPh blend are weaker than those in the P2VP/PVPh blends. By characterization via IR and ^{13}C NMR spectra, the H-bonding interactions between the pendant pyridine group of the P2VP-*b*-PEO copolymer and phenol group of the PVPh homopolymer were found to be responsible for the positive deviation from linear T_g–composition relationship. From the extents of the measured wavenumber shifts of the OH band for the blends, the strengths of H-bonding interactions were determined to be in the decreasing order of P2VP/PVPh > P2VP-*b*-PEO/PVPh > PEO/PVPh. Thus, the PEO block unit apparently defrays the average strength of intermolecular H-bonding in the P2VP-*b*-PEO/PVPh blend owing to the relatively weaker interaction between the PEO segment of the copolymer and the PVPh homopolymer. Other than the effects of the copolymer segments on altering the average strength of interactions between the polymers, the evidence of the single, composition-dependent T_g, homogeneous morphology, and single T_1^H value of the blends from the NMR characterization together supports a logical conclusion of miscibility and phase homogeneity in the homopolymer/copolymer blends. The (P2VP/PEO)/PVPh ternary blends were also investigated. The positive deviation from the linear rule that has shown in the P2VP-*b*-PEO/PVPh blends is also found in the T_g–composition curves for the (P2VP/PEO)/PVPh blend.

Acknowledgments

This work was financially supported by a basic research grant (NSC-94 2216 E006 003) in three consecutive years from National Science Council (NSC) of Taiwan. One of the co-authors, L.-T. Lee, was sponsored by an academic exchange student/scholar program (“sandwich program”) between Germany and Taiwan (DAAD–NSC) to complete one-year training (September 2004–2005) at the laboratory of Prof. S. Förster in the University of Hamburg (Germany).

References

[1] Zhu L, Mimnaugh BR, Ge Q, Quirk RP, Cheng SZD, Thomas EL, et al. Polymer 2001;42:9121.
[2] Huang YY, Chen HL, Hashimoto T. Macromolecules 2003;36:764.
[3] Aoki H, Ito S. J Phys Chem B 2001;105:4558.
[4] Zhao JQ, Pearce EM, Kwei TK. Macromolecules 1997;30:7119.
[5] Zhang XH, Wang ZG, Muthukumar M, Han CC. Macromol Rapid Commun 2005;26:1285.
[6] McGrath KJ, Roland CM, Antonietti M. Macromolecules 2000;33:8354.
[7] He Y, Li JC, Uyama H, Kobayashi S, Inoue Y. J Polym Sci Part B Polym Phys 2001;39:2898.
[8] Andrienko D, Leon S, Delle Site L, Kremer K. Macromolecules 2005; 38:5810.
[9] Duran R, Ballauff M, Wenzel M, Wegner G. Macromolecules 1988;21: 2897.
[10] Marquardt J, Thomann R, Thomann Y, Heinemann J, Mulhaupt R. Macromolecules 2001;34:8669.
[11] Ho RM, Chang CC, Chung YW, Chiang YW, Wu JY. Polymer 2003; 44:1459.
[12] Hsu JY, Nandan B, Chen MC, Chiu FC, Chen HL. Polymer 2005;46: 11837.
[13] Coleman MM, Painter PC. Prog Polym Sci 1995;20:1.
[14] Landry MR, Massa DJ, Landry CJT, Teegarden DM, Colby RH, Long TE, et al. J Appl Polym Sci 1994;54:991.
[15] Lee LT, Woo EM. Polym Int 2004;53:1813.
[16] Lee LT, Woo EM. J Polym Sci Part B Polym Phys 2006;44:1339.
[17] Vivas de Meftahi M, Frechet JMJ. Polymer 1988;29:477.
[18] Dai J, Goh SH, Lee SY, Siow KS. Polym J 1994;26:905.
[19] Wang J, Cheung MK, Mi Y. Polymer 2001;42:3087.
[20] Förster S, Khandpur AK, Zhao J, Bates FS, Hamley IW, Ryan AJ, et al. Macromolecules 1994;27:6922.
[21] Khandpur AK, Förster S, Bates FS, Hamley IW, Ryan AJ, Bras W, et al. Macromolecules 1995;28:8796.
[22] Förster S, Plantenberg T. Angew Chem Int Ed 2002;41:689.
[23] Bauer A, Hauschild S, Stolzenburg M, Förster S, Mayer C. Chem Phys Lett 2006;419:430.
[24] Hauschild S, Borchert U, Lipprandt U, Rank A, Schubert R, Förster S. Small 2005;1:1177.
[25] Lee LT. Analyses of miscibility and interactions in blends of poly(4-vinyl phenol) with aryl polyesters or block copolymers of amphiphilic segments. PhD thesis. Department of Chemical Engineering, Natl' Cheng Kung University, Taiwan; 2006.
[26] Kwei TK. J Polym Sci Polym Lett Ed 1984;22:307.
[27] Kuo SW, Chang FC. Macromolecules 2001;34:5224.
[28] Pedrosa P, Pomposo JA, Calahorra E, Cortazar M. Macromolecules 1994; 27:102.
[29] Lee JY, Painter PC, Coleman MM. Macromolecules 1988;21:954.
[30] Lin-Vien D, Colthup NB, Fateley WG, Grasselli JG. The handbook of infrared and Raman characteristic frequencies of organic molecules. Boston: Academic Press; 1991.
[31] Moskala EJ, Varnell DF, Coleman MM. Polymer 1985;26:228.
[32] Mcbrierty VJ, Douglass DC. J Polym Sci Macromol Rev 1981;16:295.
[33] Clauss J, Schmidt-Rohr KWH. Acta Polym 1993;44:1.